Benchmark for the FVCA8 Conference Finite volume methods for the Stokes and Navier-Stokes equations

F. Boyer[*]and P. Omnes[†]

September 21, 2016

The most recent version of this document, as well as all the up-to-date information on the benchmark, is available on the GitHub repository

https://github.com/FranckBoyer/FVCA8_Benchmark

We also refer to the website of the FVCA8 conference for further information on registration, submission of proceedings, etc ...

https://indico.math.cnrs.fr/event/1299/page/5

1 Introduction

1.1 Presentation

The aim of this benchmark is to compare various finite volume space discretization for the equations of incompressible fluid mechanics. We are particularly interested in evaluating accuracy, robustness, complexity and the ability to handle various families of unstructured meshes, in 2D and in 3D.

We mention that the present benchmark is the third of a series organised at the occasion of FVCA conferences:

- Benchmark on 2D anisotropic diffusion problems, FVCA5, 2008, see [6].

- Benchmark on 3D anisotropic diffusion problems, FVCA6, 2011, see [4].

It is specified that participants are free to choose only a part of the test cases. All significant contributions will be considered for publication.

1.2 The set of equations

According to the value of θ and χ below, we shall consider the steady ($\theta = 0$) or unsteady ($\theta = 1$) incompressible Stokes ($\chi = 0$) or Navier-Stokes ($\chi = 1$) equations

$$\theta \boldsymbol{u}_t - \nu \Delta \boldsymbol{u} + \chi (\boldsymbol{u} \cdot \nabla) \boldsymbol{u} + \nabla p = \mathbf{f}, \qquad (t, \mathbf{x}) \in (0, T] \times \mathcal{D},$$

$$\nabla \cdot \boldsymbol{u} = 0, \qquad (t, \mathbf{x}) \in (0, T] \times \mathcal{D},$$

$$\int_{\mathcal{D}} p(t, \mathbf{x}) d\mathbf{x} = 0, \qquad t \in (0, T]$$

$$(\text{if } \theta = 1) \ \boldsymbol{u}(0, \mathbf{x}) = \boldsymbol{u}_0(\mathbf{x}), \qquad \mathbf{x} \in \mathcal{D}$$

---

[*]Institut de Mathématiques de Toulouse, UMR 5219, Université Paul Sabatier Toulouse 3, 31962 Toulouse Cedex 9, France. Email : franck.boyer@math.univ-toulouse.fr

[†]CEA-Saclay, DEN, DM2S, STMF, LMSF, F-91191 Gif-sur-Yvette, France. Email : pascal.omnes@cea.fr

that model the motion of a viscous incompressible fluid under the action of external forces.

The domain $\mathcal{D}$ will always be the unit square or the unit cube, the final time T and the boundary conditions will be specified in the various test-cases below. Boundary conditions will always be Dirichlet (either homogeneous or not) conditions on the velocity.

1.3   The meshes

Since one of the aims of this benchmark is to assess the capacity of recent schemes to handle various types of meshes, in particular non conforming ones, we propose several families of meshes[1] that are available in the following folder of the Benchmark's GitHub repository
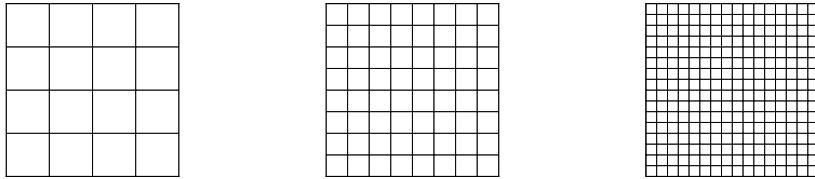
   `https://github.com/FranckBoyer/FVCA8_Benchmark/tree/master/Meshes/`

The format of the files are described in the `README.md` files respectively in the `2D` and `3D` folders.
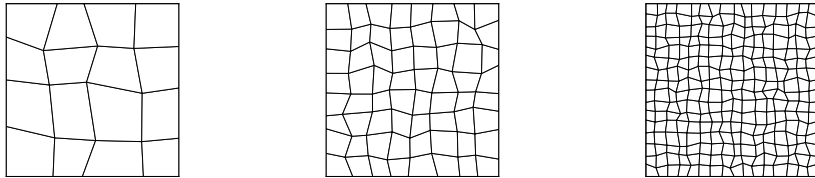
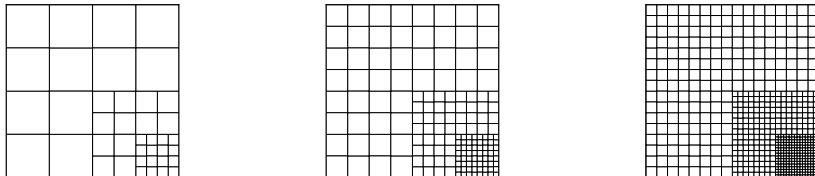- 2D triangular meshes : `mesh_tri_i` for $i \in \{1, ..., 6\}$
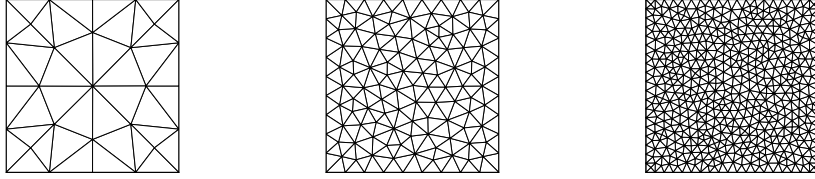
- 2D uniform Cartesian meshes : `mesh_cart_i` for $i \in \{1, ..., 7\}$

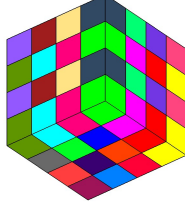- 2D quadrangles meshes : `mesh_quad_i` for $i \in \{1, ..., 7\}$

- 2D locally refined Cartesian meshes : `mesh_quad_i` for $i \in \{1, ..., 5\}$

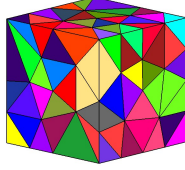

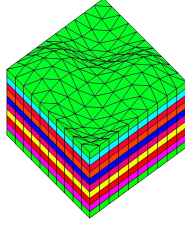[1]mostly taken from the previous FVCA5 and FVCA6 benchmarks.

- 3D hexahedral meshes : `mesh_hexa_i` for $i \in \{1, ..., 5\}$

- 3D tetrahedral meshes : `mesh_tetra_i` for $i \in \{0, ..., 6\}$

- 3D prismatic meshes : `mesh_prism_i` for $i \in \{1, ..., 4\}$

1.4   Expected outputs

Each time an exact solution is known (Sections 2 to 4), the participants will verify the accuracy and order of convergence of the schemes on the given families of meshes. Some estimation of the complexity of the schemes will also be provided.

The choice of the time-integration scheme and of the time-step in the unsteady tests is left to the participants but should be clearly indicated. Participants should also indicate the way they solve the non-linearity of the equations (Newton iterations for example), and how many such non-linear iterations were needed to reach the presented results, as well as the stopping criterion of such iterations.

More precisely, for each test case in sections 2, 3 and 4, tables like Tab. 1 and Tab. 2 should be filled with the following quantities (one complexity table for each mesh family, and one accuracy table for each value of the viscosity coefficient and each mesh family):

Accuracy table

- **i** : Number of the mesh in the mesh family. Quantities below will be labeled by i with reference to the mesh number. Growing i means finer meshes.

- **errgu** $= \left[\frac{\int_{\mathcal{D}} |\nabla(\boldsymbol{u} - \boldsymbol{u}_{\mathrm{ex}})|^2}{\int_{\mathcal{D}} |\nabla \boldsymbol{u}_{\mathrm{ex}}|^2} \right]^{1/2}$ (for $\theta = 0$) or $\left[\frac{\int_0^T \int_{\mathcal{D}} |\nabla(\boldsymbol{u} - \boldsymbol{u}_{\mathrm{ex}})|^2}{\int_0^T \int_{\mathcal{D}} |\nabla \boldsymbol{u}_{\mathrm{ex}}|^2} \right]^{1/2}$ (for $\theta = 1$) or any other quantity, to be specified by the participants, quantifying the error in the velocity derivatives L^2 norm.

- **ordgu** $= -d \frac{\ln(\mathbf{errgu}_i) - \ln(\mathbf{errgu}_{i-1})}{\ln(\mathbf{nuu}_i) - \ln(\mathbf{nuu}_{i-1})}$, where $d = 2$ or 3 is the space dimension, and **nuu** is the number of velocity unknowns.

- **erru** $= \left[\frac{\int_{\mathcal{D}} |\boldsymbol{u} - \boldsymbol{u}_{\mathrm{ex}}|^2}{\int_{\mathcal{D}} |\boldsymbol{u}_{\mathrm{ex}}|^2} \right]^{1/2}$ (for $\theta = 0$) or $\left[\frac{\int_0^T \int_{\mathcal{D}} |\boldsymbol{u} - \boldsymbol{u}_{\mathrm{ex}}|^2}{\int_0^T \int_{\mathcal{D}} |\boldsymbol{u}_{\mathrm{ex}}|^2} \right]^{1/2}$ (for $\theta = 1$), or any other quantity, to be specified by the participants, quantifying the error in the velocity L^2 norm.

- **ordu** $= -d \frac{\ln(\mathbf{erru}_i) - \ln(\mathbf{erru}_{i-1})}{\ln(\mathbf{nuu}_i) - \ln(\mathbf{nuu}_{i-1})}$, where $d = 2$ or 3 is the space dimension, and **nuu** is the number of velocity unknowns.

- **errp** $= \left[\frac{\int_{\mathcal{D}} |p - p_{\mathrm{ex}}|^2}{\int_{\mathcal{D}} |p_{\mathrm{ex}}|^2} \right]^{1/2}$ (for $\theta = 0$) or $\left[\frac{\int_0^T \int_{\mathcal{D}} |p - p_{\mathrm{ex}}|^2}{\int_0^T \int_{\mathcal{D}} |p_{\mathrm{ex}}|^2} \right]^{1/2}$ (for $\theta = 1$), or any other quantity, to be specified by the participants, quantifying the error in the pressure L^2 norm.

- **ordp** $= -d \frac{\ln(\mathbf{errp}_i) - \ln(\mathbf{errp}_{i-1})}{\ln(\mathbf{npu}_i) - \ln(\mathbf{npu}_{i-1})}$, where $d = 2$ or 3 is the space dimension, and **npu** is the number of pressure unknowns.

- **errdivu** $= \left[\int_{\mathcal{D}} |\nabla \cdot \boldsymbol{u}|^2 \right]^{1/2}$ (for $\theta = 0$) or $\left[\int_0^T \int_{\mathcal{D}} |\nabla \cdot \boldsymbol{u}|^2 \right]^{1/2}$ (for $\theta = 1$) or any other quantity, to be specified by the participants, quantifying the error in the velocity divergence L^2 norm. This quantity will be useful to measure mass conservation violation, especially for penalized methods.

- **orddivu** $= -d \frac{\ln(\mathbf{errdivu}_i) - \ln(\mathbf{errdivu}_{i-1})}{\ln(\mathbf{nuu}_i) - \ln(\mathbf{nuu}_{i-1})}$, where $d = 2$ or 3 is the space dimension, and **nuu** is the number of velocity unknowns. This order of convergence is meaningful only if **errdivu** is different from zero.

mesh	errgu	ordgu	erru	ordu	errp	ordp	errdivu	orddivu
1								
2								
. . .								

Table 1: Sample accuracy table.

Complexity table

- **nuu** : Number of velocity unknowns.

- **npu** : Number of pressure unknowns.

- **nnzu** : Number of non-zero terms in the velocity – velocity matrix.

- **nnzp** : Number of non-zero terms in the pressure – pressure matrix (for penalized methods)

- **nnzup** : Number of non-zero terms in the velocity/pressure matrix.

mesh	nuu	npu	nnzu	nnzp	nnzup
1					
2					
. . .					

Table 2: Sample complexity table.

2 Steady Stokes tests

2.1 The 2D Bercovier-Engelman test case

One of the interests of this quite classical test case is that the gradient part of the source term is small compared to the curl part, and thus it is interesting to check whether a numerical method will capture the pressure correctly.

2.1.1 Exact solution

$\boldsymbol{u}_{\text{ex}} = (u_1(x, y), -u_1(y, x))^T$ with $u_1(x, y) = -256x^2(x - 1)^2 y(y - 1)(2y - 1)$ and $p_{\text{ex}} = (x - 1/2)(y - 1/2)$

2.1.2 Parameters

$\mathcal{D} = [0, 1]^2$, $\theta = 0$, $\chi = 0$, homogeneous Dirichlet boundary conditions,
$\mathbf{f} = (f_1(x, y) + (y - 1/2), -f_1(y, x) + (x - 1/2))^T$
with $f_1(x, y) = 256 \left[x^2(x - 1)^2(12y - 6) + y(y - 1)(2y - 1)(12x^2 - 12x + 2) \right]$.
Viscosity: $\nu = 1$

2.2 3D Taylor Green Vortex

This is a widely explored test-case in the non-linear unsteady setting because, with a quite simple initial condition, it enables to study vortex dynamics, transition to turbulence, turbulent decay and energy dissipation. However, the initial velocity profile has also been used as a simple analytic solution for testing numerical methods for the Stokes system.

2.2.1 Exact solution

$$\boldsymbol{u}_{\text{ex}} = \left(\begin{array}{c} -2\cos(2\pi x)\sin(2\pi y)\sin(2\pi z) \\ \sin(2\pi x)\cos(2\pi y)\sin(2\pi z) \\ \sin(2\pi x)\sin(2\pi y)\cos(2\pi z) \end{array} \right)$$

and $p_{ex} = -6\pi \sin(2\pi x)\sin(2\pi y)\sin(2\pi z)$

2.2.2 Parameters

$\mathcal{D} = [0, 1]^3$, $\theta = 0$, $\chi = 0$, non homogeneous Dirichlet boundary conditions, $\nu = 1$ and $\mathbf{f} = (-36\pi^2 \cos(2\pi x)\sin(2\pi y)\sin(2\pi z), 0, 0)^T$.

3 Steady Navier-Stokes tests and robustness with respect to viscosity coefficient value

The exact solution here is a simple vortex that balances the pressure gradient, and the solution does not depend on the value of the viscosity. The aim of the test is to verify the behavior of the numerical solution for decreasing values of the viscosity coefficient.

3.1 Steady 2D tests

3.1.1 Exact solution

$\boldsymbol{u}_{\text{ex}} = (y, -x)^T$ and $p_{\text{ex}} = \frac{1}{2}(x^2 + y^2) - \frac{1}{3}$

3.1.2 Parameters

$\mathcal{D} = [0,1]^2$, $\theta = 0$, $\chi = 1$, non homogeneous Dirichlet boundary conditions, $\mathbf{f} = \mathbf{0}$.
Viscosity: $\nu = 10^{-1}$, $\nu = 10^{-2}$ and $\nu = 10^{-3}$.

3.2 Steady 3D tests

3.2.1 Exact solution

$\boldsymbol{u}_{\mathrm{ex}} = (y - z, z - x, x - y)^T$ and $p_{\mathrm{ex}} = (x^2 + y^2 + z^2) - xy - xz - yz - \frac{1}{4}$

3.2.2 Parameters

$\mathcal{D} = [0,1]^3$, $\theta = 0$, $\chi = 1$, non homogeneous Dirichlet boundary conditions, $\mathbf{f} = \mathbf{0}$.
Viscosity: $\nu = 10^{-1}$, $\nu = 10^{-2}$ and $\nu = 10^{-3}$.

4 Unsteady Navier-Stokes tests

4.1 Unsteady 2D tests

4.1.1 Exact solution

Let us define $\psi = e^{-5\nu\pi^2 t}\cos(\pi x)\cos(2\pi y)$. Then:
$\boldsymbol{u}_{\mathrm{ex}} = (\psi_y, -\psi_x)$ and $p_{\mathrm{ex}} = -\frac{1}{4}e^{-10\nu\pi^2 t}\pi^2(4\cos(2\pi x) + \cos(4\pi y))$.

4.1.2 Parameters

$\mathcal{D} = [0,1]^2$, $\theta = 1$, $\chi = 1$, $T = \frac{1}{10\nu}$, non homogeneous Dirichlet boundary conditions,
$\mathbf{f} = \mathbf{0}$ and $\boldsymbol{u}(t = 0) = \boldsymbol{u}_{\mathrm{ex}}(t = 0)$.
Viscosity: $\nu = 10^{-1}$ and $\nu = 10^{-2}$.

4.2 Unsteady 3D tests

4.2.1 Exact solution (generalized Beltrami flow)

$$\boldsymbol{u}_{\mathrm{ex}} = e^{38\nu t}\begin{pmatrix} e^{2x-5y-5z}(-2e^{x+7z} + 3e^{8y}) \\ e^{-5x+2y-5z}(-2e^{7x+y} + 3e^{8z}) \\ e^{-5x-5y+2z}(-2e^{7y+z} + 3e^{8x}) \end{pmatrix},$$

$$p_{\mathrm{ex}} = \frac{19}{5}e^{76\nu t}\left(5e^{-3(x+y+z)}(e^{8x+y} + e^{8y+z} + e^{x+8z}) + \sinh 2 + \sinh 3 - \sinh 5\right)$$

4.2.2 Parameters

$\mathcal{D} = [0,1]^3$, $\theta = 1$, $\chi = 1$, $T = \frac{1}{20\nu}$, inhomogeneous Dirichlet boundary conditions,
$\mathbf{f} = \mathbf{0}$ and $\boldsymbol{u}(t = 0) = \boldsymbol{u}_{\mathrm{ex}}(t = 0)$.
Viscosity: $\nu = 10^{-1}$ and $\nu = 10^{-2}$.

5 Robustness with respect to the invariance property

The solutions of the incompressible Navier–Stokes equations verify a fundamental invariance property, if the boundary conditions are independent of the pressure (e.g., pure homogeneous or non-homogeneous Dirichlet boundary conditions for $\boldsymbol{u}$): If $(\boldsymbol{u}, p)$ is solution of the equations with right-hand side $\mathbf{f}$, then $(\boldsymbol{u}, p+\psi)$ is solution of the equations with right-hand side $\mathbf{f} + \nabla\psi$.

The aim of this test is to verify if a given discretization verifies this property or how far it deviates from it.

5.1 Test on the 2D steady Stokes system

By linearity of the Stokes equations, this test amounts to verify that, for homogeneous Dirichlet conditions on the velocity field, if $\mathbf{f} = \nabla\psi$, then $\mathbf{u} = \mathbf{0}$ and $p = \psi$. We propose to test this by choosing $\psi(x, y) = \exp(-10(1 - x + 2y))$, for which the local refinement of the third 2D mesh family in the bottom right corner should play a positive role on the accuracy of the computations. This test should be performed for $\nu = 10^{-1}$ and $\nu = 10^{-2}$.

5.2 Test on the 2D steady Navier-Stokes system

For the complete Navier-Stokes equations, we propose to use the lid driven cavity tests of section 6. More precisely, we will choose $\nu = \frac{1}{400}$ and for any given mesh we shall compare the solution obtained without source term to the one obtained with a source term $\mathbf{f} = \nabla\psi$ and the same $\psi = \exp(-10(1 - x + 2y))$ as before. This will create an artificial pressure gradient in the source term whose magnitude is comparable to the *natural* pressure gradient in the cavity.

5.3 Expected outputs

Let $(\boldsymbol{u}_0, p_0)$ be the solution obtained with right-hand side $\mathbf{f} = \mathbf{0}$ and $(\boldsymbol{u}_\psi, p_\psi)$ the solution obtained with a right-hand side $\mathbf{f} = \nabla\psi$. In each case, a comparison table like the sample table Tab. 3 should be filled with the following quantities

Comparison table

- **i** : Number of the mesh in the mesh family.

- **devgu** $= \left[\int_{\mathcal{D}} |\nabla \boldsymbol{u}_\psi|^2 \right]^{1/2}$ (for Section 5.1) or $\left[\frac{\int_{\mathcal{D}} |\nabla(\boldsymbol{u}_\psi - \boldsymbol{u}_0)|^2}{\int_{\mathcal{D}} |\nabla \boldsymbol{u}_0|^2} \right]^{1/2}$ (for section 5.2) or any other quantity, to be specified by the participants, quantifying the deviations in the velocity derivatives L^2 norm.

- **codgu** $= d \frac{\ln(\textbf{devgu}_i) - \ln(\textbf{devgu}_{i-1})}{\ln(\textbf{nuu}_i) - \ln(\textbf{nuu}_{i-1})}$, where $d = 2$ or 3 is the space dimension, and **nuu** is the number of velocity unknowns.

- **devu** $= \left[\int_{\mathcal{D}} |\boldsymbol{u}_\psi|^2 \right]^{1/2}$ (for Section 5.1) or $\left[\frac{\int_{\mathcal{D}} |\boldsymbol{u}_\psi - \boldsymbol{u}_0|^2}{\int_{\mathcal{D}} |\boldsymbol{u}_0^2|} \right]^{1/2}$ (for section 5.2) or any other quantity, to be specified by the participants, quantifying the deviations in the velocity L^2 norm.

- **codu** $= d \frac{\ln(\textbf{devu}_i) - \ln(\textbf{devu}_{i-1})}{\ln(\textbf{nuu}_i) - \ln(\textbf{nuu}_{i-1})}$, where $d = 2$ or 3 is the space dimension, and **nuu** is the number of velocity unknowns.

- **devp** $= \left[\frac{\int_{\mathcal{D}} |p_\psi - \Pi\psi|^2}{\int_{\mathcal{D}} |\psi|^2} \right]^{1/2}$ (for Section 5.1) or $\left[\frac{\int_{\mathcal{D}} |p_\psi - p_0 - \Pi\psi|^2}{\int_{\mathcal{D}} |p_0 + \psi|^2} \right]^{1/2}$ (for section 5.2) or any other quantity, to be specified by the participants, quantifying the deviations in the pressure L^2 norm, and where $\Pi\psi$ is some projection of ψ to be specified by the participants.

- **codp** $= d \frac{\ln(\textbf{devp}_i) - \ln(\textbf{devp}_{i-1})}{\ln(\textbf{npu}_i) - \ln(\textbf{npu}_{i-1})}$, where $d = 2$ or 3 is the space dimension, and **npu** is the number of pressure unknowns.

mesh	devgu	codgu	devu	codu	devp	codp
1						
2						
...						

Table 3: Sample comparison table.

6   2D Lid driven cavity tests

Lid driven cavity examples are very popular since they contain many real flows features while being posed in a simple geometry. Since no exact solution is known for such flows, we rely here on the numerous results and discussions published for instance in [1, 2, 3, 5, 8, 7].

6.1   Setup

We set $\mathcal{D} = [0,1]^2$, $\theta = 0$ and $\chi = 1$ (full steady Navier-Stokes equations). There are no-slip conditions at the boundaries $x = 0$, $x = 1$, and $y = 0$: there, $\boldsymbol{u} = (0,0)^T$ is imposed. The velocity at $y = 1$ is chosen to be $\boldsymbol{u} = (1,0)^T$. Notice that, in [2], the authors choose $\boldsymbol{u} = (-1,0)^T$ at $y = 1$ to ensure that the primary vortex is positive. Of course, this choice simply modifies the results by symmetry.
For this setting, it is recognized in the literature that stable steady-state solutions exist up to a critical Reynolds number, which is located around $\nu \approx \frac{1}{8000}$.
We propose here to compare the results obtained for $\nu = \frac{1}{100}$, $\nu = \frac{1}{400}$, $\nu = \frac{1}{1000}$ and $\nu = \frac{1}{5000}$ with the available results in the literature.

- On the uniform Cartesian meshes `mesh_cart_*`, the comparisons will be quite easy since most of the available reference results are given for such grids (and obtained in general with quite high order schemes).

- We propose to perform also the computations on the non uniform grids `mesh_tri_*` and `mesh_quad_*` to investigate whether or not the method can be expected to be robust and accurate in more general geometric situations for which Cartesian grids are not available.

- Finally, we propose to use the locally refined grid `mesh_ref_*` that should be adapted to an improved accuracy of the computation around the secondary vortex (that appears in the lower right corner of the cavity, at least for high Reynolds numbers).

6.2   Expected outputs

For each simulation provided, one should try to give an idea of the complexity of the method, for instance by providing the kind of linear/nonlinear solver which is used and the number of iterations required to get the results.

Stream function   The participants should compute (an approximation of) the stream-function ψ defined by

$$u = \partial_y \psi, \ v = -\partial_x \psi, \ \ \psi(x,0) = 0, \ \ \forall x \in (0,1).$$

The formula used to compute ψ from the solution of the scheme has to be given.
In order to see if the primary (resp. secondary) vortex is accurately computed, the participants are asked to give the minimal (resp. maximal) value of ψ and the

coordinates of the point where those values are achieved

$$\psi_{\mathbf{max}}, \mathbf{x_{max}}, \mathbf{y_{max}}, \psi_{\mathbf{min}}, \mathbf{x_{min}}, \mathbf{x_{max}}.$$

Note that, with our choice of the boundary condition, the stream-function is negative in the primary vortex.

If the participants want to plot the computed streamlines (for instance only for the more accurate simulation), they are encouraged to use the following contour values for ψ

-1.175e-1	-1.15e-1	-1.1e-1	-1e-1	-9e-2	-7e-2	-5e-2	-3e-2	-1e-2	-3e-3
-1e-3	-3e-4	-1e-4	-3e-5	-1e-5	-3e-6	-1e-6	-1e-7	-1e-8	-1e-9
-1e-10	0	1e-10	1e-9	1e-8	1e-7	1e-6	3e-6	1e-5	3e-5
1e-4	3e-4	1e-3	3e-3	1e-2	2e-2	4e-2	6e-2	8e-2	1e-1

Table 4: Contour values to be used for the stream function

Velocities   In order to compare the velocity profiles in the computed flow, we ask the participants to report on the horizontal velocity u along the vertical line passing through the center of the cavity, that is $y \mapsto u(0.5, y)$, and the vertical velocity v along the vertical line passing through the center of the cavity, that is $x \mapsto v(x, 0.5)$. The results should be given in a table where the values of the coordinates $x_1, x_2, ...$ and $y_1, y_2, ...$ at which the velocities are computed are precised. Around 15 of such values evenly distributed in each direction should be given.

mesh name #1	y_1 $u(0.5, y_1)$	y_2 $u(0.5, y_1)$	y_3 $u(0.5, y_3)$	... ...
mesh name #2	y_1 $u(0.5, y_1)$	y_2 $u(0.5, y_1)$	y_3 $u(0.5, y_3)$	... ...

Table 5: Sample table for the horizontal velocity profiles.

Vorticity and Pressure   In the above references, one can also find many reference values for the pressure and vorticity fields. For concision reasons, we do not ask the participants for such values. However, they are free to give them if they find that it is of some particular interest. In such a case, one can use for instance the pressure/vorticity contour lines values given in [2].

References

[1] O. Botella and R. Peyret. Benchmark spectral results on the lid-driven cavity flow. *Computers & Fluids*, 27(4):421–433, may 1998.

[2] Charles-Henri Bruneau and Mazen Saad. The 2D lid-driven cavity problem revisited. *Computers & Fluids*, 35(3):326–348, mar 2006.

[3] Ercan Erturk. Discussions on driven cavity flow. *International Journal for Numerical Methods in Fluids*, 60(3):275–294, may 2009.

[4] Robert Eymard, Gérard Henry, Raphaèle Herbin, Florence Hubert, Robert Klfkorn, and Gianmarco Manzini. 3D benchmark on discretization schemes for anisotropic diffusion problems on general grids. In *Finite Volumes for Complex Applications VI Problems & Perspectives*, pages 895–930. Springer Science + Business Media, 2011.

[5] U Ghia, K.N Ghia, and C.T Shin. High-re solutions for incompressible flow using the navier-stokes equations and a multigrid method. *Journal of Computational Physics*, 48(3):387–411, dec 1982.

[6] Raphaèle Herbin and Florence Hubert. Benchmark on discretization schemes for anisotropic diffusion problems on general grids. In *Finite volumes for complex applications V*, pages 659–692. ISTE, London, 2008.

[7] Carlos Henrique Marchi, Roberta Suero, and Luciano Kiyoshi Araki. The lid-driven square cavity flow: numerical solution with a 1024 x 1024 grid. *J. Braz. Soc. Mech. Sci. & Eng.*, 31(3), sep 2009.

[8] P. N. Shankar and M. D. Deshpande. Fluid mechanics in the driven cavity. *Annu. Rev. Fluid Mech.*, 32(1):93–136, jan 2000.